

# Normal and Anomalous Diffusion in Soft Lorentz Gases

Rainer Klages,<sup>1,2,3,\*</sup> Sol Selene Gil Gallegos,<sup>1</sup> Janne Solanpää,<sup>4</sup> Mika Sarvilahti,<sup>4</sup> and Esa Räsänen<sup>4</sup>

<sup>1</sup>Queen Mary University of London, School of Mathematical Sciences, Mile End Road, London E1 4NS, UK

<sup>2</sup>Institut für Theoretische Physik, Technische Universität Berlin, Hardenbergstraße 36, 10623 Berlin, Germany

<sup>3</sup>Institute for Theoretical Physics, University of Cologne, Zùlpicher Straße 77, 50937 Cologne, Germany

<sup>4</sup>Computational Physics Laboratory, Tampere University, P.O. Box 692, FI-33014 Tampere, Finland

(Dated: February 18, 2019)

Motivated by electronic transport in graphene-like structures, we study the diffusion of a classical point particle in Fermi potentials situated on a triangular lattice. We call this system a soft Lorentz gas, as the hard disks in the conventional periodic Lorentz gas are replaced by soft repulsive scatterers. A thorough computational analysis yields both normal and anomalous (super) diffusion with an extreme sensitivity on model parameters. This is due to an intricate interplay between trapped and ballistic periodic orbits, whose existence is characterized by tongue-like structures in parameter space. These results hold even for small softness showing that diffusion in the paradigmatic hard Lorentz gas is not robust for realistic potentials, where we find an entirely different type of diffusion.

The rise of new micromanipulation techniques, molecular nanodevices and nanotechnologies has fuelled the scientific interest in *small systems* [1–4]. These are objects composed of small numbers of particles far from the thermodynamic limit, which exhibit only a few relevant degrees of freedom [4]. Their microscopic equations of motion are typically highly nonlinear yielding fluctuations with macroscopic statistical properties reminiscent of interacting many-particle systems. Small systems can thus serve as a laboratory for understanding the emergence of irreversibility and complexity from chaotic dynamics [5, 6]. They become especially interesting under nonequilibrium conditions, where they exhibit macroscopic transport phenomena like diffusion. By combining nonlinear dynamics with nonequilibrium statistical physics the origin of macroscopic transport from microscopic chaos in small systems was explained by formulas expressing transport coefficients in terms of dynamical systems quantities [7–10]. Similarly irreversible entropy production was found to emerge from fractal measures [7, 8] and fractal attractors [10–12]. These results paved the way for fundamental concepts like the chaotic hypothesis generalising Boltzmann’s ergodic hypothesis [13] and fluctuation theorems generalising the second law of thermodynamics [4, 8, 9, 14].

Classical transport in small systems has a quantum mechanical analogue as electronic transport in solid-state nanodevices [15]. Recently growing interest has been attracted by periodic nanosystems such as *artificial graphene* [16] fabricated in semiconductor heterostructures [17–19] or on metallic surfaces [20, 21]. In the latter case, the electrons are confined to a honeycomb geometry by CO molecules positioned with a scanning tunneling microscope in a triangular configuration. This system exhibits the properties of graphene but in a setup that is tunable regarding, e.g., the electronic density, lattice constant, geometry, and the coupling with the environment.

Interestingly, the topology of “molecular graphene” as described above is exactly the same as one of the most

paradigmatic models in dynamical systems theory, the periodic *Lorentz gas* [7–9, 22–24]. Lorentz gases mimic the motion of classical electrons in metals. They consist of a point particle scattering elastically with fixed *hard* spheres distributed either randomly or periodically in space. Originally they were devised to reproduce Drude’s theory from microscopic dynamics [22]. In groundbreaking mathematical works Lorentz gases were shown to exhibit chaos and well-behaved transport properties [25, 26], followed by understanding diffusion in computer simulations combined with stochastic theory [20, 27, 29]. Lorentz gases thus became standard models to explain the interplay between chaos and transport: Highlights were a proof of Ohm’s law from first principles [30], the analytical and numerical calculation of Lyapunov exponents [7, 8, 12] and fractal attractors [12], as well as developing a chaotic scattering theory of transport [7]. The growing interest in graphene-like systems now brings direct technological relevance to investigate classical diffusion in *soft* Lorentz gases equipped with more realistic potentials.

The conventional two-dimensional periodic Lorentz gas is a Hamiltonian particle billiard in which a point particle of mass  $m$  performs free flights with constant velocity  $v$  between elastic collisions at hard disks of radius  $r_0$ . The centers of these disks form the nodes of a triangular lattice with lattice spacing  $2r_0 + w$ , where  $w$  denotes the smallest distance between two nearby disks. Here, following previous studies on artificial graphene [31], we introduce a *soft Lorentz gas*, where the hard disks are replaced by Fermi potentials,

$$V(\mathbf{r}) = \frac{1}{1 + \exp\left(\frac{(|\mathbf{r}| - r_0)/\sigma}{\sigma}\right)}, \quad (1)$$

with  $\sigma$  determining the softness of the potential; see Fig. 1. Related models have been used to reproduce experimental results on the magnetoresistance of electrons in semiconductor antidot lattices [32–36]. In the

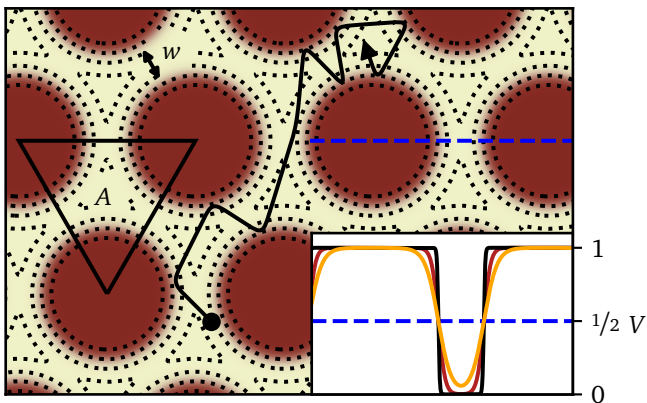


FIG. 1: The soft Lorentz gas: A point particle moves in a plane of partially overlapping Fermi potentials (inset) whose centres are situated on a triangular lattice (main figure). The dotted lines are contour lines,  $w$  denotes the minimal distance between adjacent potentials for total energy  $E = 1/2$ , and  $A$  defines a triangular unit cell. The inset shows Fermi potentials along the dashed (blue) line in the main part

for different values of the softness parameter  $\sigma$  defined in Eq. (1).

following we set  $m = r_0 = 1$  by keeping the total energy constant,  $E = 1/2$ . We thus have two control parameters,  $\sigma$  and the minimal gap size  $w$  between two nearby potentials for the given energy  $E$ . Making  $\sigma$  smaller we approach the hard scatterer limit of the conventional Lorentz gas. A crucial question is to which extent chaotic diffusion in the hard Lorentz gas [7–9, 22–24, 30] is robust by softening the potential, i.e., for more realistic models. In this Letter we show that even a slight softening introduces substantial additional complexity leading to entirely new transport properties.

Our key quantity is the diffusion coefficient

$$D = \lim_{t \rightarrow \infty} \frac{\langle (\mathbf{r}(t) - \mathbf{r}(0))^2 \rangle}{4t}, \quad (2)$$

where the numerator denotes the mean square displacement (MSD) for the position  $\mathbf{r}(t)$  of a particle at time  $t$ . The angular brackets hold for an ensemble average over initial conditions. If the MSD grows linearly in time, the above limit exists and the system exhibits normal diffusion. If the MSD grows faster than linear in time this limit diverges, and the system displays superdiffusion [30]. Technical details of the simulations carried out with the Bill2D software package [38] are explained in Sec. 1 of our Supplemental Material [39], which includes Ref. [40].

Figure 2 depicts the diffusion coefficient  $D$  as a function of the gap size  $w$  between the scattering centers for a slightly softened (main part) and the hard (inset) Lorentz gas. While for the hard scatterers  $D(w)$  is monotonically increasing and looks rather smooth, in the soft model  $D$  is a non-monotonic, highly complicated function of

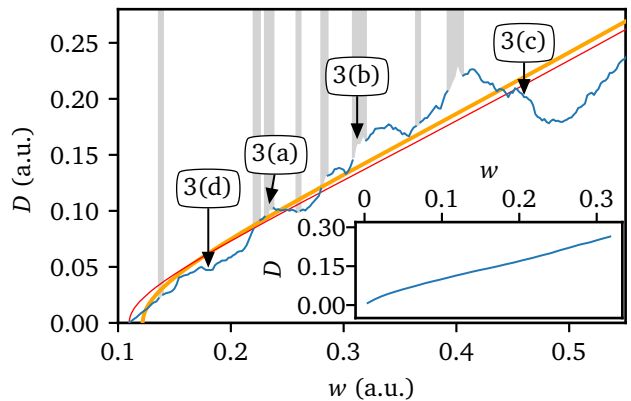


FIG. 2: Diffusion coefficient  $D$  as a function of the gap size  $w$ . The (blue) wiggled line shows simulation results for  $D(w)$  Eq. (2) in a slightly softened potential ( $\sigma = 0.05$  in Eq. (1)). The thick (orange) line represents the corresponding analytical random walk approximation  $D_B$ , the thin (red) line the numerical  $D_{B,num}$  as explained in the text. The labeled numbers 3(a) to (d) refer to the periodic orbits depicted in Fig. 3. Grey columns indicate parameter intervals in which  $D(w)$  does not exist. The inset displays  $D(w)$  obtained from simulations for the conventional hard Lorentz gas [49].

$w$ . This suggests that the diffusive properties must have changed profoundly. The diffusion coefficient for the hard Lorentz gas has been analysed in detail in previous literature, cf. Sec. 3.A in [39], which includes Refs. [18, 23–25, 41–43, 48]. Here we first explore whether there is any simple diffusion law for the soft model revealing an at least on average monotonic increase of  $D(w)$  by ignoring any fine structure. We find that a Boltzmann-type random walk approximation works well to understand the coarse functional form of  $D(w)$  [49]. For this we assume that diffusion is governed by ‘flights’ of length  $\ell_c$  during time intervals  $\tau_c$  after which a particle experiences a ‘collision’. We define a collision as an event where a particle hits the contour line of a scatterer at  $E = 1/2$  in the triangular unit cell  $A$  displayed in Fig. 1. By assuming in the spirit of Boltzmann’s molecular chaos hypothesis that all collisions are uncorrelated, the diffusion coefficient can be approximated as  $D_B(w) = \ell_c^2(w)/(4\tau_c(w))$ . In Sec. 2 of [39] we derive an analytical formula for  $D_B$  as well as an improved numerical version  $D_{B,num}$ . The results are shown as a pair of lines in Fig. 2: Both yield an approximately linear increase of  $D$  for larger  $w$ , which matches well to the coarse functional form of the simulation results. For smaller  $w$  our analytical approximation does not reproduce the onset of diffusion correctly while our improved numerical version captures it at least qualitatively well.

We now focus on the pronounced irregular fine structure of  $D(w)$  in the soft system, which is in sharp contrast to the diffusion coefficient of the hard disk model. Irregular diffusion coefficients have been re-

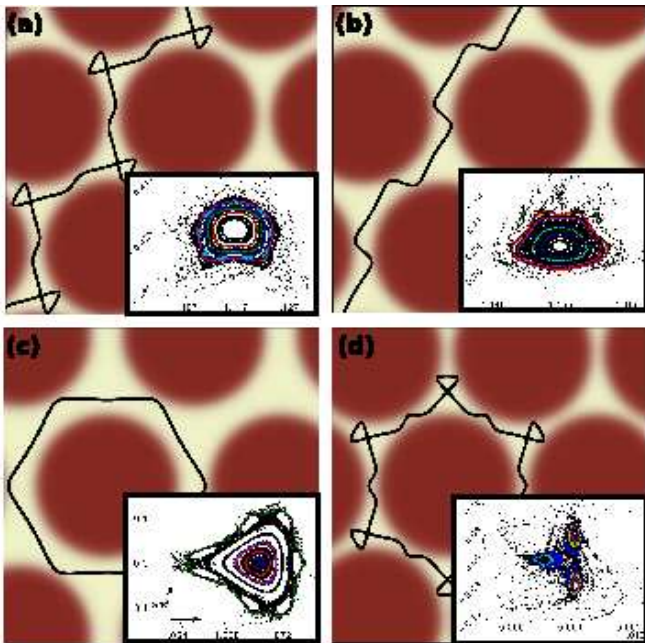


FIG. 3: Periodic orbits and islands of periodicity in phase space at different parameter values  $w$  corresponding to Fig. 2. Shown in position space are characteristic periodic orbits for (a)  $w = 0.234$ , (b)  $w = 0.31$ , (c)  $w = 0.46$ , (d)  $w = 0.18$ . (a) and (b) feature quasi-ballistically propagating orbits yielding superdiffusive parameter regions in Fig. 2 while (c) and (d) generate local minima in  $D(w)$ . The insets display associated islands of periodicity in the Poincaré surface of section phase space  $(x, \sin \theta)$  as defined in the text.

ported for parameter-dependent deterministic diffusion in much simpler chaotic dynamical systems, such as one-dimensional maps [50–53], the standard map [54, 55] and particle billiards [49, 56–58]. To our knowledge this is the first time that a diffusive fine structure has been unambiguously revealed in quite a realistic soft Hamiltonian system. For the hard Lorentz gas irregularities in  $D(w)$  also exist but are extremely tiny [49, 59], hence barely visible in Fig. 2. A second crucial difference is that our softened model generates an intricate set of superdiffusive parameter regions in which  $D(w)$  does not exist. The hard Lorentz gas displays only superdiffusion for all parameters  $w > w_\infty$  after a specific geometric transition at  $w_\infty \simeq 0.3094$  [21, 60] by exhibiting superdiffusion that is different from the soft model as discussed in Sec. 3.A of [39].

The origin of the anomalous diffusion as well as of the irregularities in  $D(w)$  of the soft Lorentz gas can be understood in terms of periodic orbits [17, 19, 52, 53, 59], as is explained by Fig. 3. It shows orbits both in position space and insets of corresponding Poincaré surfaces of section at four specific parameter values of  $w$ : Figs. 3 (a) and (b) refer to quasi-ballistically propagating periodic orbits while (c) and (d) represent localised ones. These periodic orbits exhibit different structures due to

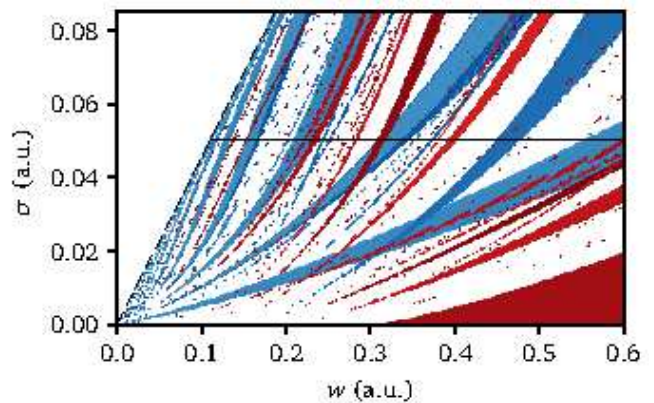


FIG. 4: Regions of periodic orbits in the parameter space of gap size  $w$  and potential softness parameter  $\sigma$ . Blue dots represent localised periodic orbits like (c), (d) in Fig. 3 while red dots correspond to quasi-ballistic orbits like (a), (b) therein. The black horizontal line at  $\sigma = 0.05$  yields a cut through the parameter space corresponding to the diffusion coefficient  $D(w)$  in Fig. 2.

different types of scattering, as is reflected in the corresponding Poincaré surfaces of section. The variables  $(x, \sin \theta)$  for the latter are defined on the boundary where a particle leaves the unit cell  $A$  in Fig. 1. Here  $x$  represents the position of the particle in a gap,  $\sin \theta$  is the angle between its velocity vector and the normal to the boundary. These islands of periodicity are typically extremely small and very difficult to detect in the whole phase space. By matching the parameter values of  $w$  for these periodic orbits to the structure of  $D(w)$  in Fig. 2 we see that the two propagating orbits correspond to two superdiffusive regions while the two localised orbits identify (approximately) two local minima in the curve. While localised orbits only slightly suppress normal diffusion without making it anomalous [50, 59, 64], islands of periodicity in phase space, also called *accelerator modes* [54, 55], generate superdiffusion [27, 28, 30, 67]. A more detailed analysis yields that all these periodic orbits are topologically extremely unstable under parameter variation: They exhibit complicated bifurcation scenarios that eventually destroy any superdiffusive window leading to parameter regions of normal diffusion before new bifurcations create new superdiffusive windows [68].

Periodic orbits thus form the backbone to understand the complicated structure of the parameter-dependent diffusion coefficient in Fig. 2. We now explore them in the full parameter space  $(w, \sigma)$ . For each point in  $(w, \sigma)$ , the numerical discovery of a localised periodic orbit or a quasi-ballistic trajectory is marked in Fig. 4 as a blue or a red dot, respectively. Interestingly, our chart reveals a very regular topological structure underlying the seemingly totally irregular curve of  $D(w)$  in Fig. 2, which lives on the horizontal black line at  $\sigma = 0.05$  in Fig. 4. We see that all periodic orbits form regular ‘tongues’ in param-

eter space which, however, we could not fit with simple functional forms like exponential, stretched exponential, or power laws. Whenever a tongue crosses the horizontal black line at  $\sigma = 0.05$  we have a local extremum in the  $D(w)$  curve of Fig. 2. Further details of this connection are described in Ref. [68]. In Sec. 3.B of [39] we explore the impact of these tongues on the diffusion coefficient under variation of  $\sigma$ . Therein we see that on a coarse scale  $D(w)$  of the hard Lorentz gas is approached continuously by decreasing  $\sigma$ , interrupted by superdiffusive regions due to quasi-ballistic tongues. This scenario is in line with a mathematical theory on the existence of elliptic islands in the phase space of closed, non-diffusive billiards that are softened [69, 70]. In these references the authors conjecture that islands are dense with respect to Lebesgue measure in parameter space for small  $\sigma$ . If this holds true one expects  $D(w)$  to be an irregular curve on arbitrarily fine scales with fractal properties [9, 50, 51, 59, 64].

In summary, we have studied diffusion under parameter variation in a soft Lorentz gas, which we put forward as a model for electronic transport in artificial graphene. We have found that the normal diffusion observed in the paradigmatic Lorentz gas with hard scatterers is not robust when softening them: Instead, the type of diffusion immediately changes dramatically generating an entirely different diffusion coefficient. This raises doubts about a universal applicability of the standard Lorentz gas for describing transport in realistic systems. In the soft Lorentz gas the diffusion coefficient turns out to be a highly irregular function under variation of control parameters with regions exhibiting superdiffusion. This is explained in terms of periodic orbits that are topologically unstable under parameter variation while exhibiting very regular structures in parameter space. Analogous results hold for varying the energy  $E$  as a parameter [68], which experimentally corresponds to changing the temperature of the system. Note that in superdiffusive parameter regions ergodicity is broken, hence for single particle experiments there will be a dependence on initial conditions [54, 55]. In real systems with thermal noise we expect these superdiffusive regions, ergodicity breaking and irregularities on fine scales to disappear, however, larger irregularities should persist under noise [56, 71]. Our results motivate to construct a more rigorous theory for calculating the diffusion coefficient curve in Fig. 2 from first principles, possibly based on generating partitions [72], which will be an extremely difficult task [9, 19]. A second crucial challenge is to test for the diffusion coefficient of Fig. 2 in experiments.

This work was supported by the Academy of Finland (grants no. 267686 and 304458). JS, MS and ER acknowledge the Finnish IT Center for Science and the Tampere Center for Scientific Computing for computational resources. SSG thanks the Mexican National Council for Science and Technology (CONACyT) for support by

scholarship no. 262481. R.K. thanks Prof. Krug (U. of Cologne), Klapp and Stark (TU Berlin) for hospitality and Profs. Turaev, Rom-Kedar and Barkai for interesting discussions. He received funding from the Office of Naval Research Global and from the London Mathematical Laboratory, where he is an External Fellow.

---

\* Electronic address: r.klages@qmul.ac.uk

- [1] C. Bustamante, J. Liphardt, and F. Ritort, *Phys. Today* **58**, 43 (2005).
- [2] F. Ritort, *Adv. Chem. Phys.* **137**, 31 (2008).
- [3] G. Radons, B. Rumpf, and H. G. Schuster, eds., *Nonlinear dynamics of nanosystems* (Wiley-VCH, Berlin, 2010).
- [4] R. Klages, W. Just, and C. Jarzynski, eds., *Nonequilibrium statistical physics of small systems: Fluctuation relations and beyond* (Wiley-VCH, Berlin, 2013).
- [5] R. Badii and A. Politi, *Complexity: hierarchical structures and scaling physics* (Cambridge University Press, Cambridge, 1997).
- [6] P. Castiglione, M. Falcioni, A. Lesne, and A. Vulpiani, *Chaos and Coarse Graining in Statistical Mechanics* (Cambridge University Press, Cambridge, 2008).
- [7] P. Gaspard, *Chaos, scattering, and statistical mechanics* (Cambridge University Press, Cambridge, 1998).
- [8] J. R. Dorfman, *An introduction to chaos in nonequilibrium statistical mechanics* (Cambridge University Press, Cambridge, 1999).
- [9] R. Klages, *Microscopic chaos, fractals and transport in nonequilibrium statistical mechanics*, (World Scientific, Singapore, 2007).
- [10] D. J. Evans and G. Morriss, *Statistical mechanics of nonequilibrium liquids* (Cambridge University Press, Cambridge, 2008), 2nd ed.
- [11] D. Ruelle, *J. Stat. Phys.* **95**, 393 (1999).
- [12] W. G. Hoover and C. G. Hoover, *Simulation and Control of Chaotic Nonequilibrium Systems* (World Scientific, Singapore, 2015).
- [13] G. Gallavotti and E. G. D. Cohen, *J. Stat. Phys.* **80**, 931 (1995).
- [14] D. J. Evans, D. J. Searles, and S. R. Williams, *Fundamentals of Classical Statistical Thermodynamics: Dissipation, Relaxation, and Fluctuation Theorems* (Wiley, Weinheim, 2016).
- [15] M. Di Ventra, *Electrical Transport in Nanoscale Systems* (Cambridge University Press, Cambridge, 2008).
- [16] M. Polini, F. Guinea, M. Lewenstein, H. C. Manoharan, and V. Pellegrini, *Nat. Nano.* **8**, 625 (2013).
- [17] M. Gibertini, A. Singha, V. Pellegrini, M. Polini, G. Vignale, A. Pinczuk, L. N. Pfeiffer, and K. W. West, *Phys. Rev. B* **79**, 241406 (2009).
- [18] E. Räsänen, C. A. Rozzi, S. Pittalis, and G. Vignale, *Phys. Rev. Lett.* **108**, 246803 (2012).
- [19] S. Wang, D. Scarabelli, L. Du, Y. Y. Kuznetsova, L. N. Pfeiffer, K. W. West, G. G. Gardner, M. J. Manfra, V. Pellegrini, S. J. Wind, et al., *Nat. Nanotech.* **13**, 29 (2018).
- [20] K. K. Gomes, W. Mar, W. Ko, F. Guinea, and H. C. Manoharan, *Nature* **483**, 306 (2012).
- [21] S. Paavilainen, M. Ropo, J. Nieminen, J. Akola, and E. Räsänen, *Nano Lett.* **16**, 3519 (2016).

- [22] H. Lorentz, Proc. Roy. Acad. Amst. **7**, 438 (1905).
- [23] D. Szasz, ed., *Hard-ball systems and the Lorentz gas*, vol. 101 of *Encyclopedia of mathematical sciences* (Springer, Berlin, 2000).
- [24] C. P. Dettmann, Comm. Theor. Phys. **62**, 521 (2014).
- [25] L. A. Bunimovich and Ya. G. Sinai, Commun. Math. Phys. **78**, 247 (1980).
- [26] L. A. Bunimovich and Ya. G. Sinai, Commun. Math. Phys. **78**, 479 (1981).
- [27] J. Machta and R. Zwanzig, Phys. Rev. Lett. **50**, 1959 (1983).
- [20] A. Zacherl, T. Geisel, J. Nierwetberg, and G. Radons, Phys. Lett. **114A**, 317 (1986).
- [29] J.-P. Bouchard and P. L. Doussal, Physica D **20**, 335 (1986).
- [30] N. I. Chernov, G. L. Eyink, J. L. Lebowitz, and Ya. G. Sinai, Phys. Rev. Lett. **70**, 2209 (1993).
- [31] M. Aichinger, S. Janecek, I. Kylänpää, and E. Räsänen, Phys. Rev. B **89**, 235433 (2014).
- [32] T. Geisel, J. Wagenhuber, P. Niebauer, and G. Obermair, Phys. Rev. Lett. **64**, 1581 (1990).
- [33] A. Lorke, J. Kotthaus, and K. Ploog, Phys. Rev. B **44**, 3447 (1991).
- [34] D. Weiss, M. Roukes, A. Menschig, P. Grambow, K. von Klitzing, and G. Weimann, Phys. Rev. Lett. **66**, 2790 (1991).
- [35] R. Fleischmann, T. Geisel, and R. Ketzmerick, Phys. Rev. Lett. **68**, 1367 (1992).
- [36] M. Fließer, G. Schmidt, and H. Spohn, Phys. Rev. E **53**, 5690 (1996).
- [30] R. Klages, G. Radons, and I. M. Sokolov, eds., *Anomalous transport: Foundations and Applications* (Wiley-VCH, Berlin, 2008).
- [38] J. Solanpää, P. Luukko, and E. Räsänen, Comp. Phys. Commun. **199**, 133 (2016).
- [39] See Supplemental Material for details.
- [40] H. Yoshida, Phys. Lett. A **150**, 262 (1990).
- [41] Ya. G. Sinai, Russ. Math. Surv. **25**, 137 (1970).
- [42] T. Gilbert and D. P. Sanders, Phys. Rev. E **80**, 041121/1 (2009).
- [43] C. Angstmann and G. Morriss, Phys. Lett. A **376**, 1819 (2012).
- [18] P. Cvitanović, J.-P. Eckmann, and P. Gaspard, Chaos, Solitons and Fractals **6**, 113 (1995).
- [23] G. Cristadoro, T. Gilbert, M. Lenci, and D. P. Sanders, Phys. Rev. E **90**, 050102 (2014).
- [24] G. Cristadoro, T. Gilbert, M. Lenci, and D. P. Sanders, Phys. Rev. E **90**, 022106 (2014).
- [25] L. Zarfaty, A. Peletskyi, I. Fouxon, S. Denisov, and E. Barkai, Phys. Rev. E **98**, 010101 (2018).
- [48] A. Lichtenberg and M. Lieberman, *Regular and chaotic dynamics*, (Springer, New York, 1992), 2nd ed.
- [49] R. Klages and C. Dellago, J. Stat. Phys. **101**, 145 (2000).
- [50] R. Klages and J. R. Dorfman, Phys. Rev. Lett. **74**, 387 (1995).
- [51] J. Groeneveld and R. Klages, J. Stat. Phys. **109**, 821 (2002).
- [52] N. Korabel and R. Klages, Phys. Rev. Lett. **89**, 214102 (2002).
- [53] N. Korabel and R. Klages, Physica D **187**, 66 (2004).
- [54] T. Manos and M. Robnik, Phys. Rev. E **89**, 022905 (2014).
- [55] M. Harsoula and G. Contopoulos, Phys. Rev. E **97**, 022215 (2018).
- [56] T. Harayama and P. Gaspard, Phys. Rev. E **64**, 036215 (2001).
- [57] T. Harayama, R. Klages, and P. Gaspard, Phys. Rev. E **66**, 026211 (2002).
- [58] L. Mátyás and R. Klages, Physica D **187**, 165 (2004).
- [59] R. Klages and N. Korabel, J. Phys. A: Math. Gen. **35**, 4823 (2002).
- [60] C. P. Dettmann, J. Stat. Phys. **146**, 181 (2012).
- [21] R. M. Feliczaki, E. Vicentini, and P. P. González-Borrero, Phys. Rev. E **96**, 052117 (2017).
- [17] P. Cvitanović, P. Gaspard, and T. Schreiber, Chaos **2**, 85 (1992).
- [19] P. Cvitanović, R. Artuso, R. Mainieri, G. Tanner, and G. Vattay, *Chaos: Classical and quantum* (Niels Bohr Institute, Copenhagen, 2007).
- [64] R. Klages and J. R. Dorfman, Phys. Rev. E **59**, 5361 (1999).
- [27] T. Geisel, A. Zacherl, and G. Radons, Phys. Rev. Lett. **59**, 2503 (1987).
- [28] T. Geisel, A. Zacherl, and G. Radons, Z. Phys. B **71**, 117 (1988).
- [67] G. Zaslavsky, Phys. Rep. **371**, 461 (2002).
- [68] S. S. Gil Gallegos, Ph.D. thesis, Queen Mary University of London (2018).
- [69] D. Turaev and V. Rom-Kedar, Nonlin. **11**, 575 (1998).
- [70] V. Rom-Kedar and D. Turaev, Physica D **130**, 187 (1999).
- [71] R. Klages, Europhys. Lett. **57**, 796 (2002).
- [72] F. Christiansen and A. Politi, Phys. Rev. E **51**, R3811 (1995).

# Supplemental Material

## 1. Technical details of the numerical simulations

The numerical simulations were carried out with the *bill2d* software package [1] for classical dynamics. The time-propagation was performed using the 4th order algorithm of Yoshida [2]. We employed a parallelogram, non-primitive unit cell containing four Fermi potentials. The full potential was represented as a sum over all Fermi potentials Eq.(1) in the unit cell and in its next and next-nearest neighboring unit cells. For the figures in the main part we performed high precision computations with an ensemble size of  $\geq 10^5$  trajectories that guaranteed a vanishingly small standard error of the mean in Eq.(2). The initial conditions were sampled uniformly in the coordinate space of the unit cell, the initial speeds of the particles were fixed to satisfy the total energy condition ( $E = 1/2$ ), and the initial launch angles were randomized. A numerical estimate for the diffusion coefficient  $D$  Eq.(2) was obtained with a linear fit to  $\langle(\mathbf{r}(t) - \mathbf{r}(0))^2\rangle$  as a function of time, where we skipped the initial transient region and instead made a fit at  $t = 1000 \dots 5000$ . The two figures shown later in this Supplement were generated with less precision than in the main part. In both cases we iterated up to time  $t = 5000$  with a time step of  $10^{-3}$ . For Fig. S1 we chose an ensemble size of 10000 particles, for Fig. S2 we had 100000 particles.

## 2. Random walk approximations for diffusion

In order to understand the coarse scale parameter dependence of the diffusion coefficient  $D(w)$  depicted in Fig. 2 we employ a Boltzmann-type random walk approximation, which was put forward in Ref. [3], see Sec. 4 therein. As briefly described in the main text, this approximation is based on the assumption that diffusion is governed by ‘flights’ of length  $\ell_c = \ell_c(w)$  over corresponding flight time intervals  $\tau_c = \tau_c(w)$  after which a particle experiences a ‘collision’. However, in contrast to the standard Lorentz gas with hard walls studied in [3] our potential is soft. Hence, here we define a collision as an event where a particle hits the contour line of a scatterer at  $E = 1/2$  in the triangular unit cell  $A$  displayed in Fig. 1 of the main text. By assuming that all collisions are uncorrelated the diffusion coefficient can be approximated as

$$D_B(w) = \frac{\ell_c^2}{4\tau_c} \quad . \quad (\text{S1})$$

In the hard Lorentz gas  $\tau_c$  can be calculated using a phase space argument analogous to the one that was put forward in Ref. [4] to compute the mean escape time  $\tau_e$  of a particle out of a unit cell. The latter can be expressed in terms of the probability to leave a trap within the time  $\tau_e$ . This quantity is in turn given by the portion of the phase space from which a particle can escape from a trap during time  $\tau_e$  divided by the total phase space volume of a trap; for details we refer to [4]. The only difference for computing  $\tau_c$  is that here one replaces the flux across the exits of a trap by the flux to the walls bounding the trap. Working this out for our soft Lorentz gas we get

$$\tau_c^{-1} = \frac{v}{A} \quad . \quad (\text{S2})$$

Here  $A = A(w)$  is the accessible area for the particle in position space, and  $v = |\mathbf{v}(w)|$  defines the average constant speed with which a particle travels between collisions. We now have everything at hand to boil down Eq.(S1) to something computable: First, using  $\ell_c = v\tau_c$  in Eq.(S1) we trivially obtain

$$D_B(w) = \frac{v^2\tau_c}{4} \quad . \quad (\text{S3})$$

Substituting  $\tau_c$  by Eq.(S2) yields

$$D_B(w) = \frac{A}{4}v \quad . \quad (\text{S4})$$

$A$  is easily computed by geometric arguments leading to our central formula

$$D_B(w) = \frac{\sqrt{3}L^2/4 - \pi r_0^2/2}{4}v \quad , \quad (\text{S5})$$

where  $L$  is the lattice spacing. It remains to calculate  $v$ . For this recall that a particle moves in the plane under the influence of overlapping Fermi potentials, see Eq.(1) in the main text. This means the kinetic energy varies depending on the position of the particle, consequently the speed fluctuates as well. However, as explained above, for Eq.(S5) we assume that a particle travels with an on average constant speed  $v$ . We define this speed in two ways by using the following approximations:

1. We calculate *analytically* an *approximate average speed*  $v_{\text{ave}} = v_{\text{ave}}(w)$  at the moment when a particle leaves  $A$ . For this we consider the contributions of the potential from two adjacent lattice points in the plane only. Without loss of generality we may choose  $(0, 0)$  and  $(L, 0)$  located at the centres of two nearby potentials  $V_1(x) := V_1(x, 0)$  and  $V_2(x) := V_2(L, 0)$  with  $L = 2r_0 + w$ . Note that with the latter equation for the lattice spacing we approximate the true gap size in the case of overlapping Fermi potentials by a gap size  $w$  derived from using a single non-overlapping Fermi potential; see Ref. [5] for details. By considering the contributions from these two potentials along the  $x$ -axis the joint potential  $V_j(x)$  reads

$$V_j(x) = V_1(x) + V_2(x) = \frac{1}{1 + \exp((|x| - r_0)/\sigma)} + \frac{1}{1 + \exp(|x - L| - r_0)/\sigma)} \quad . \quad (\text{S6})$$

We now define an average potential  $V_{\text{ave}}$  over the approximate exit of a trap according to

$$V_{\text{ave}}(w) = \frac{1}{w} \int_{r_0}^{r_0+w} V_j(x) dx \quad . \quad (\text{S7})$$

Exploiting symmetry this integral can be calculated to

$$V_{\text{ave}}(w) = 2 + \frac{2\sigma}{w} \ln \left( \frac{2}{1 + \exp(w/\sigma)} \right) \quad . \quad (\text{S8})$$

Conservation of energy yields  $v = \sqrt{2(E - V_j(x))}$ . Combining this with Eq. (S8), an average exit speed can be expressed as

$$v_{\text{ave}}(w) = \sqrt{2(E - V_{\text{ave}}(w))} \quad . \quad (\text{S9})$$

2. A second definition is based on calculating *numerically* the *correct average speed*  $v_{\text{num}} = v_{\text{num}}(w)$  while a particle is leaving a trap. Using symmetry we have to compute the integral

$$v_{\text{num}} = \frac{2}{w} \int_{r_\epsilon}^{r_\epsilon+w/2} \sqrt{2(E - V_{\text{tot}}(x))} dx, \quad (\text{S10})$$

where  $V_{\text{tot}}(x) := V_{\text{tot}}(x, 0)$  is the sum over the range of potentials as defined in Sec. I above. Note that this requires us to compute  $r_\epsilon$  defined by  $V_{\text{tot}}(r_\epsilon) = 1/2$  due to the overlapping potentials. This integral is not solvable analytically, hence we compute it numerically.

Using these two approximations for the speed  $v$  in Eq.(S5) yields our two approximations  $D_B$  and  $D_{B,\text{num}}$  plotted in Fig. 2 of the main text.

### 3. Transition between the soft and the hard Lorentz gas

In this section we discuss first qualitatively and then quantitatively the changes of the diffusive dynamics in the hard disk Lorentz gas when softening the scatterers. In Subsec. A we outline generic dynamical systems properties of both models by discussing their similarities and differences. Subsection B presents computer simulation results for the diffusion coefficient as a function of the smoothness parameter  $\sigma$  exploring this transition in more depth when  $\sigma$  is getting smaller.

#### 3.1. The hard and the soft Lorentz gas: Similarities and differences in their diffusive dynamics

Diffusion in the conventional Lorentz gas consisting of a point particle scattering with hard disks has been studied in a large number of works; see [6–10] for reviews. Pioneering mathematical research by Bunimovich and Sinai showed rigorously that the Lorentz gas is a K-system, which implies that it is mixing and ergodic [11, 12]. It is furthermore a hyperbolic chaotic dynamical system [13]. For the two-dimensional periodic Lorentz gas with scatterers situated on a triangular lattice these strong chaos properties imply that diffusion is normal in the parameter regime of the gap size  $w$  of  $0 < w < w_\infty$ , in the sense that the mean square displacement (MSD) grows linearly with time in the long-time limit, as was proven in Ref. [11]. In this regime the diffusion coefficient as a function of  $w$  was explored in Refs. [3, 4, 14–16]. The result from simulations of  $D(w)$  is shown in the inset of Fig. 2 in the main text. While in this plot  $D$  looks like a rather smooth function of  $w$  it was shown in Ref. [3] that there are irregularities in the form of slight wiggles on very fine scales. The order of magnitude of these irregularities is by far smaller than in the soft model, cp. Fig. 2 in the main text for the soft Lorentz gas with Fig. 1(b) in [3]. So far it is only known that these irregularities exist in the conventional Lorentz gas, but they could not be explained, e.g., in terms of periodic orbits. There are attempts in the literature, however, to compute  $D(w)$  for the hard periodic Lorentz gas in terms of *unstable* periodic orbits [? ? ? ].

Note that  $w_\infty = 4\sqrt{3} - 3 \simeq 0.3094$  defines the onset of an *infinite horizon* in the periodic Lorentz gas, where a particle can for the first time move ballistically along infinite channels across the entire lattice without colliding with any scatterer. Accordingly, for  $w_\infty > w$  diffusion becomes anomalous, and  $D$  as defined by Eq. (2) in the main text does not exist anymore. This is reflected in our chart of periodic orbits in Fig. 4 (main part) as the big red tongue of quasi-ballistic periodic orbits emerging from  $w \simeq 0.31$  for small  $\sigma$ . More precisely, infinite horizon Lorentz gases exhibit a special type of superdiffusion, where the MSD grows like  $t \ln t$ . This is due to a family of strictly ballistic periodic orbits which, however, occupy only zero volume in the whole phase space of the system [22? ? ? ? ].

In marked contrast to this hard Lorentz gas scenario of purely chaotic deterministic diffusion with a well-defined diffusion coefficient for  $w < w_\infty$ , and superdiffusion for  $w > w_\infty$  due to an infinite horizon, in our main text we have shown that softening the hard disks by using overlapping Fermi potentials changes the diffusive dynamics profoundly: Even a minimal softening of the potential yields a mixed phase space [26] composed of chaotic regions interrupted by small ‘islands’ of periodic orbits, cf. Fig. 3 (main part). Note that in contrast to the hard Lorentz gas these islands occupy non-zero volume and are *stable* in phase space. This implies a completely different type of non-hyperbolic dynamics compared to the well-behaved hard Lorentz gas which, in turn, is reflected in profound changes of the corresponding diffusive properties. In turn, it is well-known that islands of periodicity in phase space corresponding to ‘propagating’ periodic orbits, also called accelerator modes, lead to superdiffusion, even if they are very tiny, while parameter regions without any islands correspond to normal diffusion [29, 31? ? ? , 32].

At first view this phenomenon may look similar to the infinite horizon case in the hard periodic Lorentz gas. But in the soft model the orbits generating superdiffusion are not strictly ‘ballistic’ in the sense of being collision-free, as is demonstrated by Fig. 3 (main text). Rather particles collide with the scatterers in intricate ways while they move on average in one direction. Hence there are no infinite horizon channels in our soft system, as there is always a force acting on a particle, therefore we call these trajectories *quasi-ballistic*. Secondly, in contrast to the hard Lorentz gas the phase space of a quasi-ballistic island of periodicity is non-zero, due to the velocity now representing an additional degree of freedom. This implies a generically different type of superdiffusion compared to the hard Lorentz gas infinite horizon case with a MSD that grows like  $t^\alpha$ ,  $\alpha > 1$  [22? ? ? ? ].

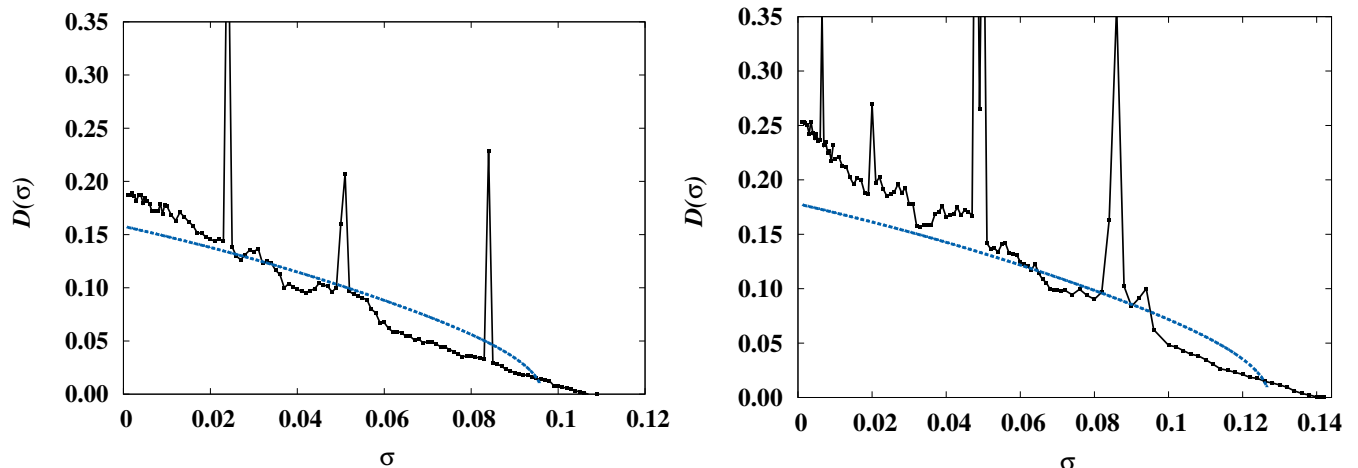
To our knowledge so far there are no works that study the transition from Hamiltonian particle billiards consisting of hard walls, like Lorentz gases, to systems consisting of soft periodic potentials, like our model, as far as diffusion is concerned. The only research we are aware of is a series of articles by Turaev and Rom-Kedar, who investigate in mathematical depth the changes of the dynamics by softening the hard walls of billiards, however, without exploring the impact on diffusive properties [33, 34]. There is a claim in these references that under softening hard walls islands of periodicity become typical in parameter space, but this has not been observed in parameter space as shown in our



Fig. 4. We also remark that the theory by Turaev and Rom-Kedar predicts that for small  $\sigma$  the tongues of periodic orbits depicted in Fig. 4 should grow linearly in parameter space, see Theorem 1 in Ref. [34]. But to verify this numerically is at present out of reach, as it is extremely difficult to find small islands of periodicity especially for  $\sigma$  close to zero.

### 3.2. The diffusion coefficient as a function of the smoothness parameter

We now explore the transition between the hard and the soft Lorentz gas regarding their diffusive properties in more depth. In the main text we have focused on the diffusion coefficient as a function of the gap size  $w$  between two adjacent scatterers for fixed smoothness parameter  $\sigma$ , cf. Fig. 2. Here we first present results for the diffusion coefficient  $D$  at fixed  $w$  under variation of  $\sigma$ . This supplements our previous analysis related to the chart of periodic orbits shown in Fig. 4, main part: While so far we have explored the parameter space displayed therein along horizontal cuts through this plane, in the following we elucidate what happens along vertical cuts. This sheds light on the transition of diffusive properties between the soft and the hard scatterer case when  $\sigma$  is close to zero.



Supplementary Figure S1: Diffusion coefficient  $D$  as a function of the smoothness parameter  $\sigma$  when the gap size is fixed to  $w = 0.235$  (left) and  $w = 0.31$  (right). The black lines with symbols represent results from computer simulations. The peaks therein correspond to parameter regions where the diffusion coefficient has not converged to a final value due to the existence of quasi-ballistic periodic orbits. The (blue) dashed lines give the simple random walk approximation  $D_{\text{MZ}}(\sigma)$  Eq. (S11).

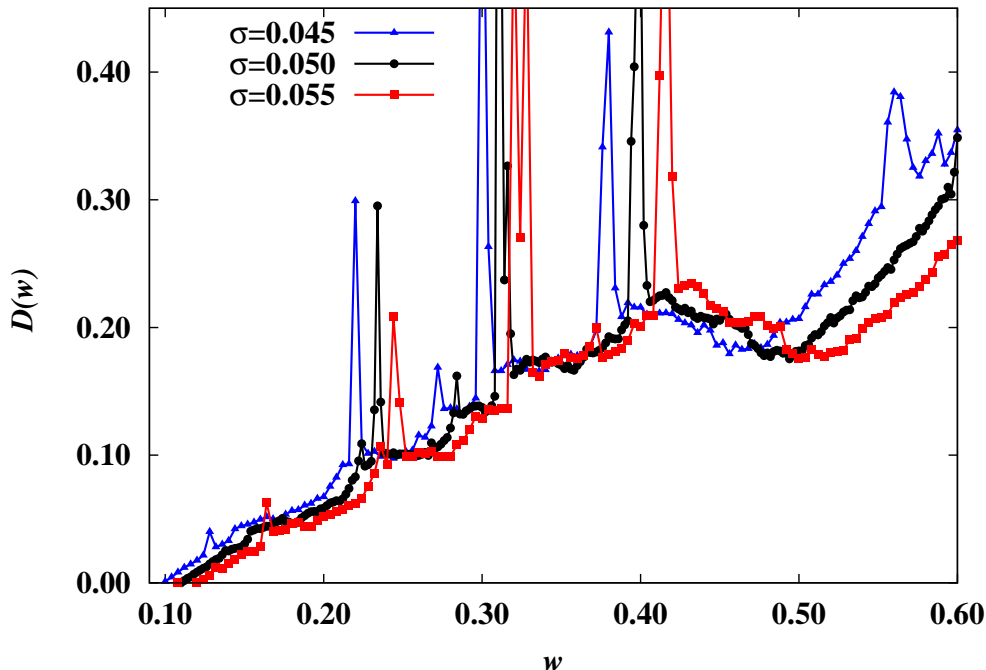
Figure S1 (a) and (b) depict results for  $D(\sigma)$  at two fixed values of  $w$ . These two figures correspond to vertical cuts in Fig. 4 (main text) from top to bottom by showing what happens when  $\sigma$  approaches zero. We see that in both cases  $D(\sigma)$  is an increasing function when decreasing  $\sigma$ . However, as in case of  $D(w)$  for fixed  $\sigma$  in Fig. 2 (main text), we observe again irregularities on finer scales. They are supplemented by peaks representing parameter regions where  $D$  has not converged to a final value, as it does not exist due to the existence of quasi-ballistic periodic orbits. These peaks match to respective quasi-ballistic tongues in Fig. 4 (main text). Note, however, that in the left figure the lowest tongue around  $\sigma \simeq 0.01$  has been missed. This may be due to the chosen spacing between two adjacent data points  $D(\sigma)$ , or that our initial ensemble did not catch a respective tiny island of stability. The values of  $D(0)$  correspond to the respective results for the hard Lorentz gas shown in the inset of Fig. 2 (main text).

The blue dashed lines are analytical results representing a simple random walk approximation put forward by Machta and Zwanzig [4], suitably adapted to the soft Lorentz gas: The assumption is that particles hop from trap to trap on a triangular lattice, cf. Fig. 1 (main text) for the trapping region  $A$  with an escape time  $\tau_e$  from each trap, where the centres of the traps are a distance  $\ell = L/\sqrt{3}$  apart. By assuming no memory between two jumps, similarly to Eq. (S1) above yielding our Boltzmann approximation the diffusion coefficient can be approximated to

$$D_{\text{MZ}}(\sigma) = \frac{\ell^2}{4\tau_e} . \quad (\text{S11})$$

Again in analogy to the Boltzmann approximation  $\tau_e$  is now given again by a phase space argument,

$$\tau_e^{-1} = \frac{3wv}{\pi A} , \quad (\text{S12})$$



Supplementary Figure S2: Diffusion coefficient  $D(w)$  obtained from simulations for three different values of the smoothness parameter  $\sigma$  as given in the figure.

where, as explained in Sec. in the Supplement, the only difference to the collision time  $\tau_c$  in Eq. (S2) is that for calculating the escape time  $\tau_e$  we consider the portion of phase space where a particle leaves a trap. Combining Eq. (S12) with Eq. (S11) by plugging in the value for  $A$  as before yields

$$D_{\text{MZ}}(\sigma) = \frac{L^2 w}{\pi(\sqrt{3}L^2 - 2\pi)} v \quad . \quad (\text{S13})$$

In Fig. S1 above we have used this formula by replacing  $v$  with the average velocity calculated in Eqs. (S8),(S9) above,  $v = v_{\text{ave}}$ , which yields the dashed blue lines. We see that this analytical random walk approximation matches qualitatively to the numerical results by particularly explaining the increase of the (normal) diffusion coefficient when the system approaches the hard Lorentz gas limit for small  $\sigma$ . Note that the quantitative mismatch between the data and the approximation is increasing from  $\sigma \rightarrow 0$ , as is analysed in detail in [3, 14]. What we can learn from Fig. S1 and its analysis is that the transition between diffusion in the soft and the hard Lorentz gas for  $\sigma$  close to zero looks smooth on a coarse grained level as far as the diffusion coefficient is concerned when it exists, as is confirmed by our random walk approximation. However, whenever quasi-ballistic islands of periodicity occur, they interrupt this scenario. Increasing the numerical precision will reveal more and more superdiffusive parameter regions, probably even an infinite set of them, thus severely disrupting any smooth transition scenario. This result is fully in line with our chart of periodic orbits Fig. 4 (main text) by illustrating it in detail for  $D(\sigma)$ .

We finish our discussion of the impact of the smoothness parameter on diffusion in the soft Lorentz gas by presenting numerical results for  $D(w)$  at three different values of  $\sigma$ , see Fig. S2. The shift of the different peaks, where diffusion is anomalous, to the left when  $\sigma$  is getting smaller is again fully in line with our chart of periodic orbits Fig. 4 (main text). We see that the whole curve where the normal diffusion coefficient exists is slightly deforming under variation of  $\sigma$ : Except in a tiny parameter region of  $0.4 < w < 0.5$  overall it is increasing when  $\sigma$  is getting smaller, i.e., when the soft system is approaching the hard Lorentz gas limit. Within the parameter region of  $0 < w < 0.31$  eventually it will converge to the known diffusion coefficient of the hard Lorentz shown in the inset of Fig. 2 (main text) while the whole parameter region for  $w > 0.31$  will gradually become superdiffusive.

---

\* Electronic address: r.klages@qmul.ac.uk

- [1] J. Solanpää, P. Luukko, and E. Räsänen, *Comp. Phys. Commun.* **199**, 133 (2016).
- [2] H. Yoshida, *Phys. Lett. A* **150**, 262 (1990).
- [3] R. Klages and C. Dellago, *J. Stat. Phys.* **101**, 145 (2000).
- [4] J. Machta and R. Zwanzig, *Phys. Rev. Lett.* **50**, 1959 (1983).
- [5] S. S. Gil Gallegos, Ph.D. thesis, Queen Mary University of London (2018).
- [6] P. Gaspard, *Chaos, scattering, and statistical mechanics* (Cambridge University Press, Cambridge, 1998).
- [7] J. R. Dorfman, *An introduction to chaos in nonequilibrium statistical mechanics* (Cambridge University Press, Cambridge, 1999).
- [8] R. Klages, *Microscopic chaos, fractals and transport in nonequilibrium statistical mechanics*, (World Scientific, Singapore, 2007).
- [9] D. Szasz, ed., *Hard-ball systems and the Lorentz gas*, vol. 101 of *Encyclopedia of mathematical sciences* (Springer, Berlin, 2000).
- [10] C. P. Dettmann, *Comm. Theor. Phys.* **62**, 521 (2014).
- [11] L. A. Bunimovich and Ya. G. Sinai, *Commun. Math. Phys.* **78**, 247 (1980).
- [12] L. A. Bunimovich and Ya. G. Sinai, *Commun. Math. Phys.* **78**, 479 (1981).
- [13] Ya. G. Sinai, *Russ. Math. Surv.* **25**, 137 (1970).
- [14] R. Klages and N. Korabel, *J. Phys. A: Math. Gen.* **35**, 4823 (2002).
- [15] T. Gilbert and D. P. Sanders, *Phys. Rev. E* **80**, 041121/1 (2009).
- [16] C. Angstmann and G. Morriss, *Phys. Lett. A* **376**, 1819 (2012).
- [17] P. Cvitanović, P. Gaspard, and T. Schreiber, *Chaos* **2**, 85 (1992).
- [18] P. Cvitanović, J.-P. Eckmann, and P. Gaspard, *Chaos, Solitons and Fractals* **6**, 113 (1995).
- [19] P. Cvitanović, R. Artuso, R. Mainieri, G. Tanner, and G. Vattay, *Chaos: Classical and quantum* (Niels Bohr Institute, Copenhagen, 2007).
- [20] A. Zacherl, T. Geisel, J. Nierwetberg, and G. Radons, *Phys. Lett.* **114A**, 317 (1986).
- [21] R. M. Feliczaki, E. Vicentini, and P. P. González-Borrero, *Phys. Rev. E* **96**, 052117 (2017).
- [22] C. P. Dettmann, *J. Stat. Phys.* **146**, 181 (2012).
- [23] G. Cristadoro, T. Gilbert, M. Lenci, and D. P. Sanders, *Phys. Rev. E* **90**, 050102 (2014).
- [24] G. Cristadoro, T. Gilbert, M. Lenci, and D. P. Sanders, *Phys. Rev. E* **90**, 022106 (2014).
- [25] L. Zarfaty, A. Peletskyi, I. Fouxon, S. Denisov, and E. Barkai, *Phys. Rev. E* **98**, 010101 (2018).
- [26] A. Lichtenberg and M. Leiberman, *Regular and chaotic dynamics*, (Springer, New York, 1992), 2nd ed.
- [27] T. Geisel, A. Zacherl, and G. Radons, *Phys. Rev. Lett.* **59**, 2503 (1987).
- [28] T. Geisel, A. Zacherl, and G. Radons, *Z. Phys. B* **71**, 117 (1988).
- [29] G. Zaslavsky, *Phys. Rep.* **371**, 461 (2002).
- [30] R. Klages, G. Radons, and I. M. Sokolov, eds., *Anomalous transport: Foundations and Applications* (Wiley-VCH, Berlin, 2008).
- [31] T. Manos and M. Robnik, *Phys. Rev. E* **89**, 022905 (2014).
- [32] M. Harsoula and G. Contopoulos, *Phys. Rev. E* **97**, 022215 (2018).
- [33] D. Turaev and V. Rom-Kedar, *Nonlinearity* **11**, 575 (1998).
- [34] V. Rom-Kedar and D. Turaev, *Physica D* **130**, 187 (1999).